An Improved Method for Incorporating Magnetic Saturation in the Q-d Synchronous Machine Model

Keith Corzine
Missouri University of Science and Technology

Brian T. Kuhn

S. D. Sudhoff

H. J. Hegner

AN IMPROVED METHOD FOR INCORPORATING MAGNETIC SATURATION IN THE Q-D SYNCHRONOUS MACHINE MODEL

K. A. Corzine Student Member, **B.T. Kuhn** Student Member, **S. D. Sudhoff**, Member and **H.J. Hegner***, Member

Department of Electrical Engineering
University of Missouri - Rolla
Rolla, Missouri 65409-0040

*Naval Surface Warfare Center
Annapolis Detachment, Caderock Division
Annapolis, Maryland 21402

Abstract **- An improved technique for incorporating saturation into the q-d axis model (Park's model) of a synchronous machine is proposed. By choosing magnetizing flux linkage as a state variable, iterative procedures required by traditional methods are avoided. The saturation function is represented by an arctangent function which has some distinct advantages over polynomial representations and look-up tables. In particular, the parameters of the proposed function all have physical significance and the proposed function is defined over an infinite range of flux linkage. The model is verified for steady-state and transient conditions using a laboratory synchronous machine - rectifier system similar to those commonly used for Naval and aerospace power generation.**

I. INTRODUCTION

Synchronous machine models must include magnetic saturation in order to accurately predict the machine performance. Finite element analysis provides an accurate method of incorporating magnetic saturation, however, the computational intensity of this method makes it impractical for computing the performance of large power systems [1]. Several authors have proposed electric circuit models derived from a simplified finite element representation of the machine geometry [2,3,4]. It is then possible to include saturation in the stator teeth and leakage paths as well as the magnetizing path. Although these models provide an accurate method of representing magnetic saturation, they present some difficulty in parameter identification requiring search coils to be mounted in various magnetic paths of the machine or finite element analysis. The q-d axis model based on Park's equations is widely used in power system analysis due to its computational efficiency [5,6]. Although not as accurate as the finite element method, the q-d model is adequate for predicting steady-state and transient synchronous machine performance for system studies. This paper proposes an improved method for incorporating magnetic saturation into the q-d axis synchronous machine model. In particular, the traditional approach uses saturation factors which leads to an iterative process [5,6,7] whereas the proposed method is completely non-iterative. Furthermore, a novel method for representing the saturation function is proposed which involves fitting the slope of the saturation curve to an arctangent function. This representation has the advantage that saturation is defined over an infinite range of flux. In addition, the saturation function is defined by only four parameters all of which have physical significance.

PE-990-EC-0-05-1997 A paper recommended and approved by the IEEE Electric Machinery Committee of the IEEE Power Engineering Society for publication in the IEEE Transactions on Energy Conversion. Manuscript submitted January 8, 1997; made available for printing May 23, 1997.

II. SYNCHRONOUS MACHINE MODEL

The synchronous machine model considered herein is based on Park's equivalent circuit and includes the provision for an arbitrary number of damper windings in each axis as illustrated in Fig. 1. The q- and d-axis voltage equations may be expressed in the rotor reference frame as [8]

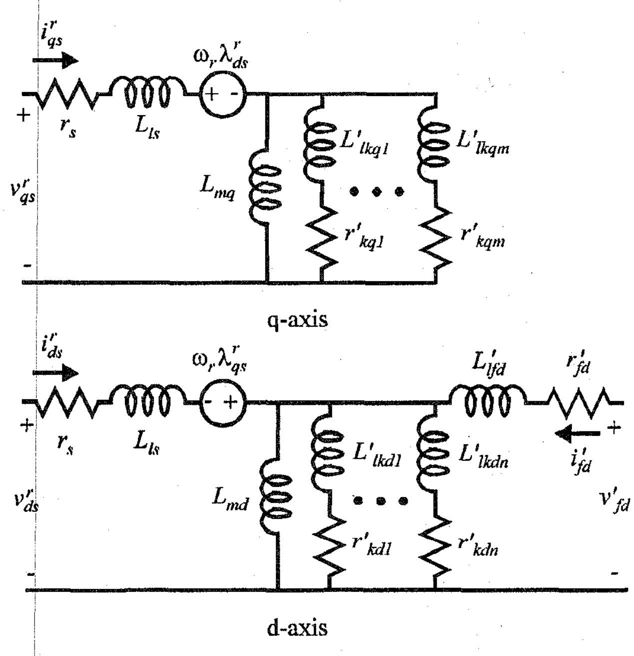

Figure 1. Synchronous machine equivalent circuit.

$$v_{qs}^r = r_s i_{qs}^r + \omega_r \lambda_{ds}^r + p\lambda_{qs}^r \quad (1)$$

$$v_{ds}^r = r_s i_{ds}^r - \omega_r \lambda_{qs}^r + p\lambda_{ds}^r \quad (2)$$

$$v_{0s} = r_s i_{0s} + p\lambda_{0s} \quad (3)$$

$$\mathbf{v}_{qr}^{\prime r} = \mathbf{r}_{qr}^{\prime} \mathbf{i}_{qr}^{\prime r} + p\Lambda_{qr}^{\prime r} \quad (4)$$

$$\mathbf{v}_{dr}^{\prime r} = \mathbf{r}_{dr}^{\prime} \mathbf{i}_{dr}^{\prime r} + p\Lambda_{dr}^{\prime r} \quad (5)$$

where

$$\mathbf{r}_{qr}^{\prime} = \begin{bmatrix} r_{kq1}^{\prime} & 0 & \cdots & 0 \\ 0 & r_{kq2}^{\prime} & \cdots & 0 \\ \vdots & \vdots & & \vdots \\ 0 & 0 & \cdots & r_{kqm}^{\prime} \end{bmatrix} \quad (6)$$

$$\mathbf{r}_{dr}^{\prime} = \begin{bmatrix} r_{fd}^{\prime} & 0 & \cdots & 0 \\ 0 & r_{kd1}^{\prime} & \cdots & 0 \\ \vdots & \vdots & & \vdots \\ 0 & 0 & \cdots & r_{kdn}^{\prime} \end{bmatrix} \quad (7)$$

and

$$\mathbf{f}_{qr}^{\prime r} = \left[f_{kq1}^{\prime r} \; f_{kq2}^{\prime r} \; \cdots \; f_{kqm}^{\prime r} \right]^T \quad (8)$$

$$\mathbf{f}_{dr}^{\prime r} = \left[f_{fd}^{\prime r} \; f_{kd1}^{\prime r} \; f_{kd2}^{\prime r} \; \cdots \; f_{kdn}^{\prime r} \right]^T . \quad (9)$$

where **f** may be voltage, current, or flux linkage and m and n are the number of damper windings used in representing the q- and d-axis circuits respectively. Herein, the rotor damper and field circuits are referred to the stator circuit by the turns ratio N_s/N_j where j may be $kq1$ through kqm, $kd1$ through kdn or fd [8]. Neglecting magnetic saturation, the flux linkages are related to the machine currents by

$$\lambda_{qs}^r = L_{ls} i_{qs}^r + \lambda_{mq}^r \quad (10)$$

$$\lambda_{ds}^r = L_{ls} i_{ds}^r + \lambda_{md}^r \quad (11)$$

$$\lambda_{0s} = L_{ls} i_{0s} \quad (12)$$

$$\Lambda_{qr}^{\prime r} = \mathbf{L}_{lqr}^{\prime} \mathbf{i}_{qr}^{\prime r} + \begin{bmatrix} 1 \\ 1 \\ \vdots \\ 1 \end{bmatrix} \lambda_{mq}^r \quad (13)$$

$$\Lambda_{dr}^{\prime r} = \mathbf{L}_{ldr}^{\prime} \mathbf{i}_{dr}^{\prime r} + \begin{bmatrix} 1 \\ 1 \\ \vdots \\ 1 \end{bmatrix} \lambda_{md}^r \quad (14)$$

where

$$\lambda_{mq}^r = L_{mq} \left(i_{qs}^r + \sum_{\text{col}} \left[\mathbf{i}_{qr}^{\prime r} \right] \right) \quad (15)$$

$$\lambda_{md}^r = L_{md} \left(i_{ds}^r + \sum_{\text{col}} \left[\mathbf{i}_{dr}^{\prime r} \right] \right) \quad (16)$$

and

$$\mathbf{L}_{lqr}^{\prime r} = \begin{bmatrix} L_{lkq1}^{\prime} & 0 & \cdots & 0 \\ 0 & L_{lkq2}^{\prime} & \cdots & 0 \\ \vdots & \vdots & & \vdots \\ 0 & 0 & \cdots & L_{lkqm}^{\prime} \end{bmatrix} \quad (17)$$

$$\mathbf{L}_{ldr}^{\prime r} = \begin{bmatrix} L_{lfd}^{\prime} & 0 & \cdots & 0 \\ 0 & L_{lkd1}^{\prime} & \cdots & 0 \\ \vdots & \vdots & & \vdots \\ 0 & 0 & \cdots & L_{lkqn}^{\prime} \end{bmatrix} . \quad (18)$$

In (15-16), $\sum_{\text{col}}$ denotes summation of all of the elements in a column vector. The electromagnetic torque may be expressed in terms of the stator currents and stator flux linkages as

$$T_e = \left(\frac{3}{2}\right)\left(\frac{P}{2}\right)\left(\lambda_{ds}^r i_{qs}^r - \lambda_{qs}^r i_{ds}^r\right) \quad (19)$$

where P is the number of poles.

It should be noted that it is possible to include the effects of mutual rotor leakage inductances or mutual rotor damper resistances by adding the appropriate terms in (6-7) and (17-18).

III. Representation of Magnetic Saturation

In this section, the synchronous machine model will be modified so as to incorporate magnetic saturation into the d-axis magnetizing path. Although q-axis saturation is common in the literature [3,6,7,8], it will be shown experimentally that neglecting q-axis saturation is sufficiently accurate for calculating power system transients involving salient machines. Iteration of the saturation function is avoided by using the d-axis magnetizing flux linkage as a state variable instead of the d-axis stator flux linkage. In order to construct a model with the d-axis magnetizing flux linkage as a state variable it is necessary to formulate an expression for the time derivative of the magnetizing flux linkage in terms of input variables and the remaining state variables. The first step in finding such an expression is to write the d-axis magnetizing current in terms of the magnetizing flux linkage as

$$i_{md}^{r}(\lambda_{md}^{r}) = F(\lambda_{md}^{r}) \,. \tag{20}$$

From (14), the d-axis rotor current vector may be expressed

$$\mathbf{i}_{dr}^{\prime r} = \left[\mathbf{L}_{ldr}^{\prime r}\right]^{-1}\left(\Lambda_{dr}^{\prime r} - \begin{bmatrix}1\\1\\\vdots\\1\end{bmatrix}\lambda_{md}^{r}\right) . \tag{21}$$

The d-axis stator current can be written as the difference of the magnetizing current and the sum of the rotor currents

$$i_{ds}^{r} = i_{md}^{r} - \sum_{\text{col}} \mathbf{i}_{dr}^{\prime r} \,. \tag{22}$$

Using (21) and (22) to calculate the d-axis stator and rotor currents allows the derivatives of the d-axis rotor flux linkages and the d-axis stator flux linkages to be calculated using the d-axis voltage equations. The derivation proceeds by substitution of (20) and (21) into (22) which yields

$$i_{ds}^{r}(\lambda_{md}^{r}) = F(\lambda_{md}^{r}) - \sum_{\text{col}}\left\{\left[\mathbf{L}_{ldr}^{\prime r}\right]^{-1}\left(\Lambda_{dr}^{\prime r} - \begin{bmatrix}1\\1\\\vdots\\1\end{bmatrix}\lambda_{md}^{r}\right)\right\} . \tag{23}$$

The d-axis stator flux linkage may be expressed by substituting (23) into (10)

$$\lambda_{ds}^{r} = L_{ls}F(\lambda_{md}^{r}) - L_{ls}\sum_{\text{col}}\left[L_{ldr}^{\prime r}\right]^{-1}\left[\Lambda_{dr}^{\prime r}\right] + \cdots$$
$$+ L_{ls}\sum_{\text{col}}\left[\mathbf{L}_{ldr}^{\prime r}\right]^{-1}\begin{bmatrix}1\\1\\\vdots\\1\end{bmatrix}\lambda_{md}^{r} + \lambda_{md}^{r} \tag{24}$$

Taking the time derivative of (24) yields

$$p\lambda_{ds}^{r} = L_{ls}\frac{\partial F}{\partial \lambda_{md}^{r}}p\lambda_{md}^{r} - L_{ls}\sum_{\text{col}}\left[\mathbf{L}_{ldr}^{\prime r}\right]^{-1}p\left[\Lambda_{dr}^{\prime r}\right] + \cdots$$
$$+ L_{ls}\sum_{\text{col}}\left[\mathbf{L}_{ldr}^{\prime r}\right]^{-1}\begin{bmatrix}1\\1\\\vdots\\1\end{bmatrix}p\lambda_{md}^{r} + p\lambda_{md}^{r} \,. \tag{25}$$

Solving (25) for the time derivative of the d-axis magnetizing flux linkage yields

$$p\lambda_{md}^{r} = \frac{p\lambda_{ds}^{r} + L_{ls}\sum_{\text{col}}\left[\mathbf{L}_{ldr}^{\prime r}\right]^{-1}p\left[\Lambda_{dr}^{\prime r}\right]}{1 + L_{ls}\frac{\partial F}{\partial \lambda_{md}^{r}} + L_{ls}\sum_{\text{col}}\left[\mathbf{L}_{ldr}^{\prime r}\right]^{-1}\begin{bmatrix}1\\1\\\vdots\\1\end{bmatrix}} \,. \tag{26}$$

The procedure for calculating the derivative of the d-axis state variables is as follows. First, the d-axis stator and rotor currents are calculated using (21) and (22). These currents are then used in conjunction with the d-axis voltage equations to calculate the time derivatives of the d-axis stator and rotor flux linkages. Note, however, that the time derivative of the stator flux linkage is not integrated since the stator flux linkage is not being used as a state variable. Finally, the derivatives of the d-axis flux linkages are used in conjunction with (26) to determine the derivative of the d-axis magnetizing flux linkage which is a state variable.

Although the model derivation presented herein only represents saturation in the d-axis, it is possible to account for magnetic saturation in the q-axis by using the q-axis magnetizing flux linkage as a state variable and writing an expression similar to (26). This method of accounting for q-axis saturation is only approximate, however, since the machine saturation depends on the combination of q- and d-axis flux (cross coupling effect).

IV. Representation of The Saturation Function

The relationship between the magnetizing flux linkage and magnetizing current is linear for both unsaturated and highly saturated conditions, although the slopes and intercepts of the two regions are different. The slope of this characteristic is therefore initially constant, undergoes a transition, and finally becomes constant again. Thus, it is reasonable to expect that the slope of the saturation function could be represented by the arctangent function. In particular,

$$\frac{\partial F(\lambda^r_{md})}{\partial \lambda^r_{md}} = \frac{2}{\pi} M_d \arctan\left(\tau_T(\lambda^r_{md} - \lambda_T)\right) + M_a \qquad (27)$$

where M_d and M_a are related to the initial and final slopes of the saturation function by

$$M_d = \frac{M_f - M_i}{2} \qquad (28)$$

$$M_a = \frac{M_f + M_i}{2}\,. \qquad (29)$$

In (27) τ_T defines the tightness of the transition from initial slope to final slope with respect to λ^r_{md} and λ_T defines the point of transition. Integration of (27) subject to the constraint that zero magnetizing current corresponds to zero magnetizing flux linkage yields

$$F(\lambda^r_{md}) = \frac{2M_d}{\pi}\left[(\lambda^r_{md} - \lambda_T)\arctan\left(\tau_T(\lambda^r_{md} - \lambda_T)\right) - \lambda_T \arctan(\tau_T \lambda_T)\right] + \frac{M_d}{\pi \tau_T}\left[\ln\left(1 + \tau_T^2 \lambda_T^2\right) - \ln\left(1 + \tau_T^2 (\lambda^r_{md} - \lambda_T)^2\right)\right] + M_a \lambda^r_{md}\,. \qquad (30)$$

In practice, (30) yields and excellent fit to the observed characteristic, as is illustrated in Fig. 2. Therein the saturation function representation based on (30) is compared to measured laboratory data. As can be seen, there is an excellent correspondence. From the model development it can be shown that the magnetizing flux linkage and current in Fig. 2 can be determined from the open circuit line-to-line rms voltage $V_{LL,oc}$ versus field current $i_{fd,oc}$ by

$$\lambda^r_{md} = \sqrt{\frac{2}{3}}\,\frac{V_{LL,oc}}{\omega_{r,oc}} \qquad (31)$$

$$i^r_{md} = \frac{2}{3}\frac{N_{fd}}{N_s} i_{fd,oc} \qquad (32)$$

where $\omega_{r,oc}$ is the electrical rotor speed in rad/sec used in the open circuit test.

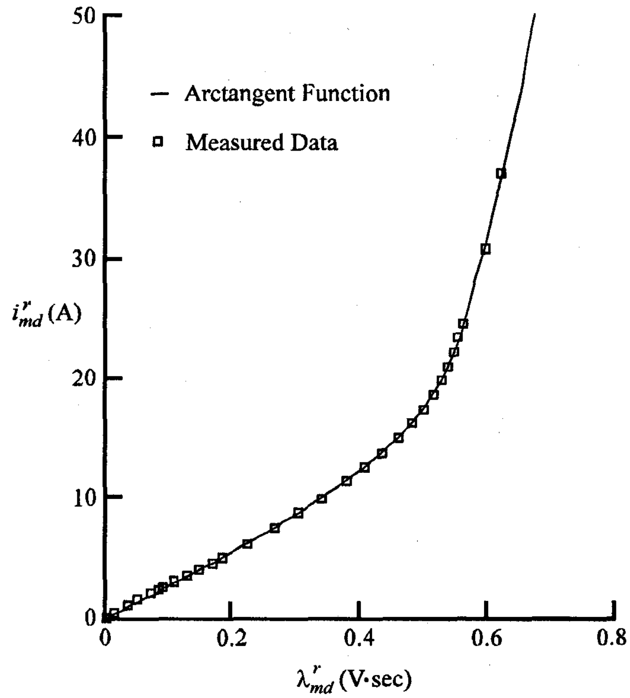

Figure 2. Measured and arctangent function saturation curves

The approach taken here has distinct advantages over other approaches such as incorporating the saturation characteristic as a table lookup function or representation of the saturation function as a polynomial series. Advantages over the table look-up approach are that (*i*) (30) is defined over a larger (infinite) operating range than is represented in the original data, (*ii*) the convenience of specifying the entire curve with four parameters, and (*iii*) no noise in estimating the derivative. Advantages over the polynomial method include (*i*) infinite range of applicability (all polynomial representations eventually break down), and (*ii*) all of the parameters of this approach have physical meaning such as initial slope, final slope, breakpoint, and tightness of breakpoint.

V. SATURATION MODEL VERIFICATION

Figure 3 depicts the test system used to verify the synchronous machine saturation model. The synchronous machine parameters, obtained using standstill frequency response and the open circuit voltage characteristic, are listed in Table I. The dc link inductor has an inductance of 1.19 mH and a series resistance of 0.32 Ω, and r_1 and r_2 were 66.11 Ω and 57.9 Ω respectively. Figure 4 illustrates the transient behavior of the system operated at an electrical speed of 377 rad/sec with a fixed field voltage of 25.45 V as the switch is closed. Variables depicted include the field

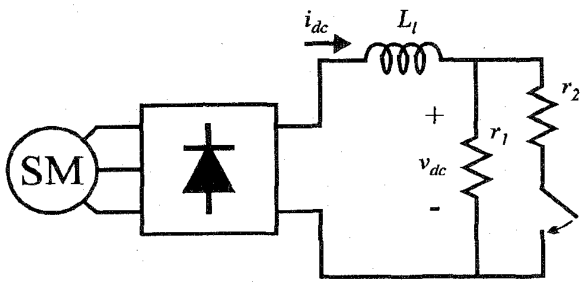

Figure 3. Configuration for stepped load test.

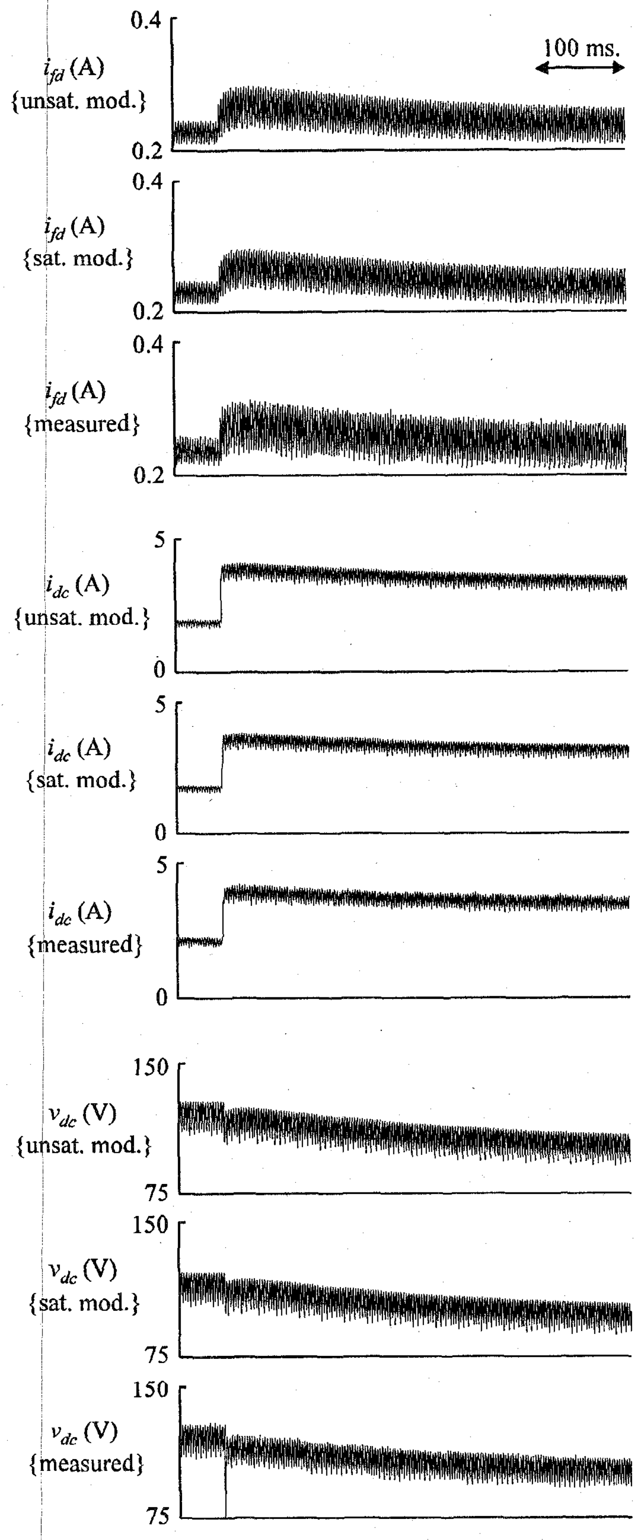

Figure 4. System performance during a step change in load (low field current).

current, the dc link current, and the dc load voltage as predicted by a model which does not include saturation, the proposed saturation model, and laboratory measurements. As can be seen, immediately following the closing of the switch, the dc link current rises quite rapidly and the dc voltage drops. The field current rises in order to maintain constant flux in the machine. As the field and damper winding currents decay, the flux level in the machine drops; this reduces the back emf which in turn causes the dc current and voltage to decrease. Since the field current is low, the machine is operating in the unsaturated portion of the saturation curve. Thus, there is no difference between the model including saturation and the model neglecting saturation. Both models adequately predict the transient response when compared to the laboratory measurements.

Figure 5 demonstrates the system response to a step change in load with the field voltage set to 104.8 V. In this experiment, the measured referred field resistance drifted slightly from the previous experiment to 0.135 Ω. The load resistances r_1 and r_2 also changed slightly to 67.03 Ω and 57.9 Ω respectively. In this study, the operation is at a point beyond the knee of the saturation curve as can be seen by comparing the steady-state (prior to switch closing) and transient responses of the models neglecting and including saturation. This difference in model prediction is most evident in the dc current and voltage. It can be seen that the model including saturation adequately predicts the steady-state and transient responses observed in the laboratory.

Table I. 3.7 kW SYNCHRONOUS MACHINE PARAMETERS

$r_s = 0.382\ \Omega$	$L_{ls} = 0.83$ mH	$L_{mq} = 13.5$ mH	
$r'_{kd1} = 40.47\ \Omega$	$L'_{lkd1} = 4.73$ mH	$r'_{kq1} = 31.8\ \Omega$	$L'_{lkq1} = 6.13$ mH
$r'_{kd2} = 1.31\ \Omega$	$L'_{lkd2} = 3.68$ mH	$r'_{kq2} = 0.923\ \Omega$	$L'_{lkq2} = 3.4$ mH
$r'_{fd} = 0.122\ \Omega$	$L'_{lfd} = 2.54$ mH	$N_s/N_{fd} = 0.0271$	$P = 4$
$M_a = 142.9$ 1/H	$M_d = 122.5$ 1/H	$\lambda_T = 0.545$ V•sec	$\tau_T = 26.48$ 1/V•sec

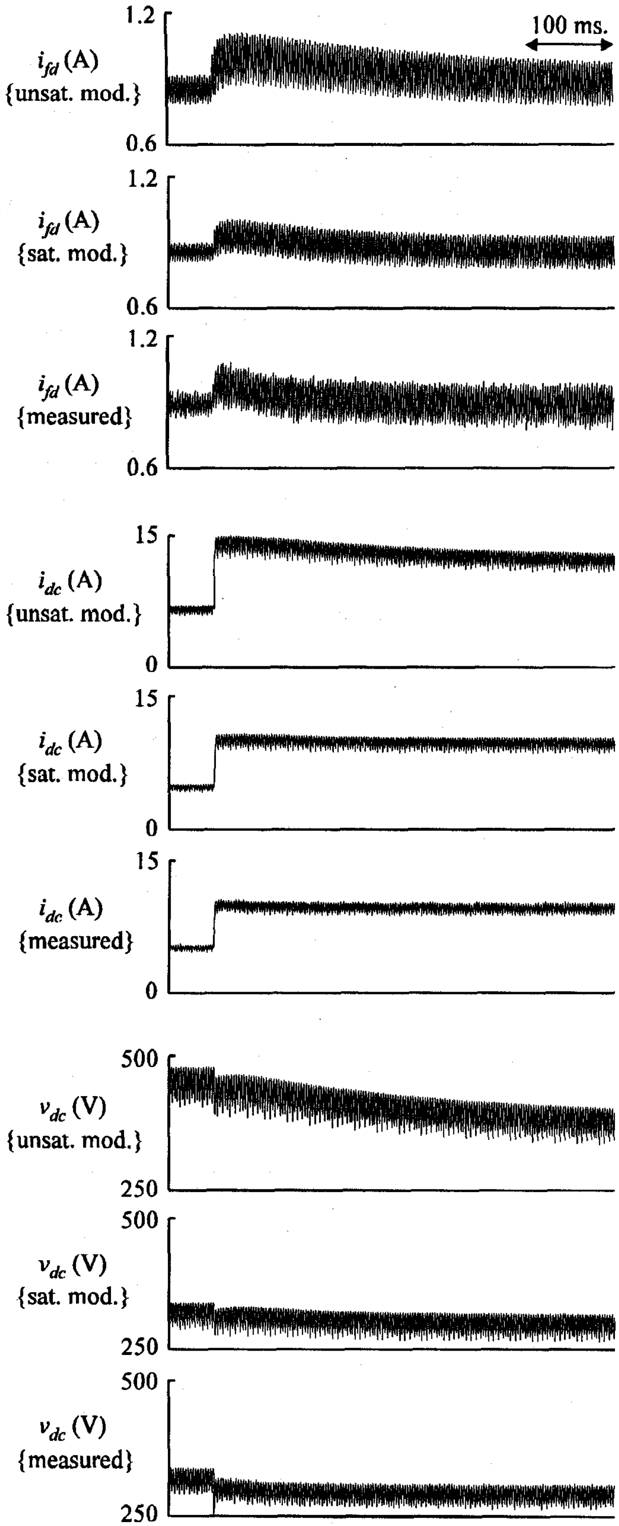

Figure 5. System performance during a step change in load (high field current).

VII. Conclusion

A new method of including saturation in the q-d axis model of a synchronous machine is proposed. The new method is not iterative as are traditional approaches. In addition, the saturation function is represented by an arctangent function with only four parameters. The parameters are related to the slope and change in slope of the saturation function and thus have a more significant meaning than the parameters of a polynomial fit. This representation also eliminates the noise in estimating the saturation function derivative that occurs with a table look-up approach. Moreover, the saturation function is applicable for an infinite range of flux. The proposed saturation model is shown to be adequate in predicting the performance of a synchronous machine/rectifier system.

VIII. Acknowledgments

The authors would like to acknowledge the Naval Surface Warefare Center for support of this project.

IX. References

[1] F. Piriou, and A Razek, "A Model for Coupled Magnetic-Electric Circuits in Electric Machines With Skewed Slots", *IEEE Transactions on Magnetics*, vol. 26, no. 2, March 1990, pp. 1096-1100.

[2] J.O. Ojo and T.A. Lipo, "An Improved Model for Saturated Salient Pole Synchronous Motors", *IEEE Transactions on Energy Conversion*, vol. 4, no. 1, March 1989, pp. 135-142.

[3] I. Boldea and S.A. Nasar, "A General Equivalent Circuit (GEC) of Electric Machines", *IEEE Transactions on Energy Conversion*, vol. 3, no. 3, September 1988, pp. 689-695.

[4] G.R. Slemon, "An Equivalent Circuit Approach to Analysis of Synchronous Machines With Saliency and Saturation", *IEEE Transactions on Energy Conversion*, vol. 5, no. 3, September 1990, pp. 538-545.

[5] C.H. Thomas, Discussion of "Analogue Computer Representation of Synchronous Generators in Voltage-Regulation Studies", *Transactions of AIEE* (Power Apparatus and Systems), vol. 75, December 1956, pp. 1182-1184.

[6] R.G. Harley, D.J.N. Limebeer, and E. Chirricozzi, "Comparative Study of Saturation Methods in Synchronous Machine Models", *IEE Proceedings*, vol. 127, Part B, no. , January 1980, pp. -7.

[7] K. Hirayama, "Practical Detailed Model for Generators", *IEEE Transactions on Energy Conversion*, vol. 10, no. , March 1995, pp. 105-110.

[8] P. C. Krause, O. Wasynczuk, S.D. Sudhoff, *Analysis of Electric Machinery*, IEEE Press, 1995.

Keith A. Corzine received the BSEE and MSEE degrees from the University of Missouri - Rolla in 1992 and 1994, respectively, and is currently pursuing the Ph.D. degree. His interest include the design and modeling of electric machinery and electric drive systems.

Brian T. Kuhn received the BSEE degree from the University of Missouri - Rolla in 1996 and is currently pursuing the MS degree. His interest include modeling of switched reluctance motors and resonant converters.

Scott D. Sudhoff received the BSEE, MSEE, and Ph.D. degrees at Purdue University in 1988, 1989, and 1991, respectively. He is currently an Assistant Professor at the University of Missouri - Rolla. His interest include the analysis, simulation, and design of electric machinery, drive systems, and finite-inertia power systems. He has authored or co-authored over twenty-five papers in these areas.

Henery J. Hegner received the BSEE degree from Virginia Polytechnical Institute and State University in 1983 and the MSEE degree from Purdue University in 1992. Mr. Hegner is employed within the Electrical Systems Department of the Machines Research and Development Directive at the Naval Surface Warfare Center in Annapolis, Maryland.